Radiation tolerance of Fe-Cr-Al alloys for accident-tolerant fuel cladding applications

SAND2017-9377D

Samuel A. Briggs
Sandia National Laboratories

Research Motivation

- Fe-Cr-Al-based alloys continue to be investigated as candidate materials for accident-tolerant fuel (ATF) cladding applications due primarily to their excellent high-temperature corrosion and oxidation resistance
  - Demonstrates superior performance in the steam environments of loss-of-coolant accident (LOCA) conditions by forming a passive Al_2O_3 scale in contrast to Zr-based alloys currently in service, which tend to exacerbate accidents by oxidizing exothermically and producing H_2 gas[1]
- High-Cr ferritic systems typically face problems with radiation-induced hardening and embrittlement due to the formation of dislocation loops and α′ phase precipitates under LWR-relevant conditions
  - Fe-Cr-Al forms $a\langle 100\rangle$ and ${}^{a}/_{2}\langle 111\rangle$ dislocation loops typical of other ferritic systems
  - α′ precipitation normally occurs after long-term thermal aging in Fe-based alloys with Cr contents over 9 at.% at temperatures below 475 °C[2]
  - Kinetics of precipitation are typically slow - radiation has been shown to accelerate the formation of this phase
- Comprehensive understanding of radiation tolerance is critical in order to design an optimized Fe-Cr-Al-based alloy composition & microstructure for ATF cladding applications
  - Requires understanding of composition, dose, and temperature effects on radiation response, in addition to investigation of oxide dispersion-strengthened (ODS) variants

Research Goals

- **Determine how α′ precipitation response is affected by varying Cr and Al contents and irradiation dose**
- **Investigate precipitate stability and dissolution kinetics during annealing at elevated temperatures**
- **Study dislocation loop microstructures in ODS Fe-Cr-Al variants as a function of irradiation temperature**

Experimental

Samples

- Four conventional Fe-Cr-Al model alloys plus ODS variant
- Fabrication route:
  - **Conventional**
    Arc-melted → heat-treated → hot forged/rolled → cold-rolled (10% reduction)[3]
  - **ODS**
    Ball-milled (40hrs) → degassed → hot extruded[4]
- ~20-50 µm grain size (conventional)
- ~100-300 nm grain size (ODS)

Table 1: *Fe-Cr-Al alloy compositions in at.%.*

Alloy	Fe	Cr	Al	Y	O	C	Si	N
Fe-10Cr-9.3Al	bal.	**10.15**	9.34	0.023	<0.01	0.022	<0.02	<0.01
Fe-12Cr-8.7Al	bal.	**12.16**	8.66	0.016	<0.01	0.022	0.02	<0.01
Fe-15Cr-7.7Al	bal.	**15.33**	7.70	0.021	<0.01	0.022	0.02	<0.01
Fe-18Cr-5.8Al	bal.	**18.00**	5.81	0.010	<0.01	0.022	<0.02	<0.01
125YF ODS	bal.	**11.79**	9.21	0.112	0.63	0.087	0.02	0.08

**S, and P contents at or below 10 ppm*

Irradiation Campaign

- SS-J2 tensile specimens for each composition were loaded capsules and irradiated in the High-Flux Isotope Reactor (HFIR)
- Temperature was determined by using passive SiC thermometry

Figure 1: *Image of disassembled irradiation capsule designed for exposure of specimens in HFIR.*

Table 2: *Irradiation conditions for each irradiation capsule in HFIR.*

Capsule ID	Exposure Time (hrs)	Neutron Flux (n/cm²s) E > 0.1 MeV	Neutron Fluence (n/cm²) E > 0.1 MeV	Dose Rate (dpa/s)	Dose (dpa)	Irradiation Temperature (°C)
FCAY-01	120	8.54×10^{14}	3.69×10^{20}	7.7×10^{-7}	0.3	334.5±0.6
FCAY-02	301	8.54×10^{14}	9.25×10^{20}	7.7×10^{-7}	0.8	355.1±3.4
FCAY-03	614	8.84×10^{14}	1.95×10^{21}	8.1×10^{-7}	1.8	381.9±5.4
FCAY-04	2456	8.74×10^{14}	7.73×10^{21}	7.9×10^{-7}	7.0	319.9±10.2
FCAT-01	590	1.10×10^{15}	2.17×10^{21}	9.8×10^{-7}	1.9	194.5 ± 37.9
FCAT-02	590	1.04×10^{15}	2.17×10^{21}	9.3×10^{-7}	1.8	363.6 ± 23.1
FCAT-03	590	1.10×10^{15}	2.17×10^{21}	9.8×10^{-7}	1.9	559.4 ± 28.1

Results

Atom Probe Tomography Analysis

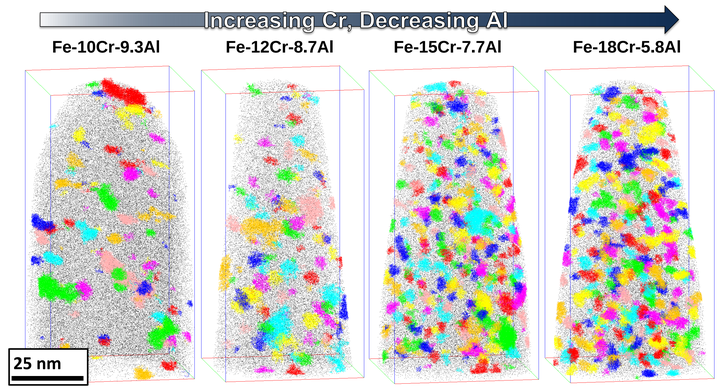

Figure 2: *Comparison of precipitate morphologies in the four Fe-Cr-Al compositions irradiated to 7 dpa at 320 °C. α′ precipitates indexed by the cluster finding algorithm are uniquely colored. Black atoms represent 2% of the detected Fe atoms; regions-of-interest are 50×50×100 nm.*

- **All APT specimens prepared from irradiated specimens by focused ion beam (FIB)**
- **Precipitate density scales with increasing Cr, decreasing Al content, larger precipitates observed in lower Cr specimens**
- **Precipitate volume fraction saturates and coarsening regime initiates by 1.8 dpa as radius increases while density decreases (not shown)**
- **APT data corroborated by ex-situ SANS analysis**

Small-Angle Neutron Scattering Analysis

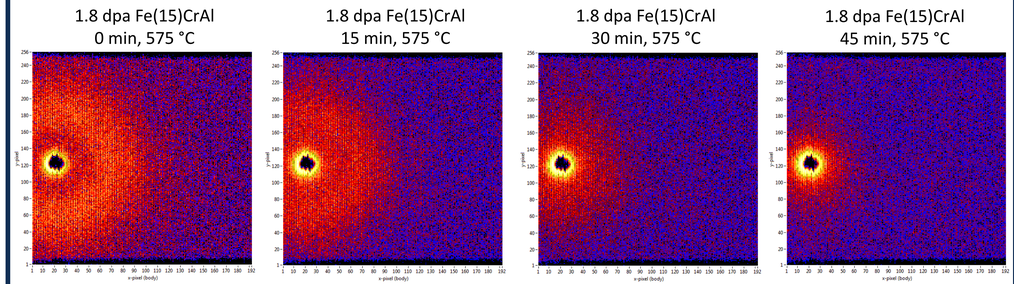

Figure 3: *Time progression of SANS diffractograms for 1.8 dpa Fe-15Cr-7.7Al during in-situ annealing at 575 °C. α′ precipitate signal manifests as an orange ring in the raw data, which is shown to fade and disappear over a 45 minute anneal.*

- **SANS diffractograms were collected during in-situ annealing of 1.8 dpa neutron-irradiated Fe-Cr-Al specimens at various temperatures above α′ phase boundary**
- **Large differences in precipitate dissolution kinetics are observed for temperatures between 500 and 575 °C (not shown)**

Scanning Transmission Electron Microscopy Analysis

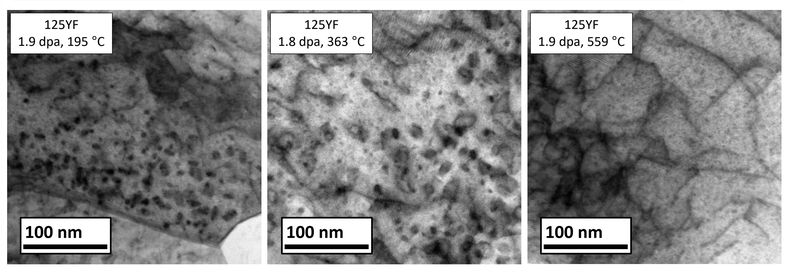

Figure 4: *Dislocation loop microstructures in 125YF ODS Fe-Cr-Al variant following neutron irradiation to ~1.9 dpa at various temperatures. Imaged using BF-STEM on $\langle 100\rangle$ zone axis.*

- **Specimens prepared via FIB, loops imaged using bright-field STEM on $\langle 100\rangle$ zone axis[5]**
- **Higher densities of small loops observed for lower irradiation temperatures**
- **No loops observed following irradiation at 559 °C**

- **Large reactive element oxide particles are shown to decorate grain boundaries in ODS Fe-Cr-Al**
- **Smallest nanoparticles are not resolved by conventional STEM/EDS measurements – more data processing required (MVSA)**
- **Nanoparticles appear stable under LWR-relevant neutron irradiation conditions**

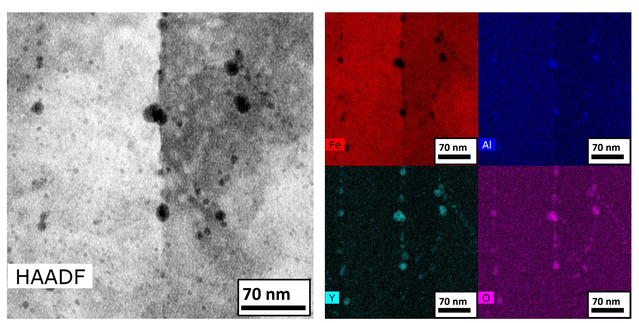

Figure 5: *Typical STEM/EDS spectral images showing typical ODS nanoparticle structures neutron-irradiated 125YF. Image shown for 1.9 dpa, 195 °C condition.*

Discussion

- α′ precipitation is observed in all irradiated Fe-Cr-Al specimens and Cr content of α′ precipitates in Fe-Cr-Al ranges from ~63-88 at.% - clusters in alloys with increased Al content are less enriched in Cr when compared to the ~85 at.% Cr precipitates observed in binary Fe-Cr
  - Al is seen to be rejected from the α′ phase (not shown), suggesting that Al shifts the α-α′ phase boundary
- Precipitate morphology evolution agrees with predictions based on the Lifshitz, Slyozov and Wagner (LSW) power law model for diffusion-limited coarsening[6] (See Figures 6 & 7)
- SANS with in-situ annealing demonstrates that precipitates dissolve rapidly at temperatures above the α-α′ phase boundary
- Temperature plays a large role in dislocation loop morphology, and higher densities of much smaller loops are seen in ODS Fe-Cr-Al variants compared to conventional alloys[7]

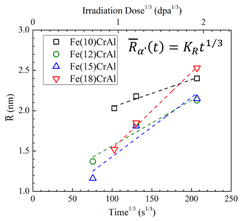

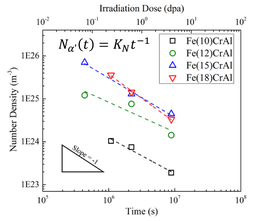

Figures 6 & 7: *SANS results demonstrate good agreement with trends predicated by LSW coarsening models.*

(left) Average radius increases with $t^{1/3}$.

(right) Number density is inversely proportional to dose/time at temperature.

Conclusions

- Precipitation response is sensitive to alloy composition and irradiation conditions
  - ↑ in Cr ∝ ↑ in α′ num. density & ↑ in α′ diameter
  - ↑ in dpa ∝ ↓ in α′ num. density & ↑ in α′ diameter
  - Al additions result in decreased Cr enrichment in α′ precipitates – could have impact on precipitate hardening contribution
- α′ precipitation is a diffusion-limited phenomena
  - Coarsening mechanism in irradiated material is similar to thermally-aged system
- Precipitates won't impact alloy performance in LOCA scenarios
- ODS microstructure appears stable under LWR-relevant neutron irradiation conditions, and significantly effect the defect structure following irradiation

Future Work

- Investigate effects of other minor solute elements
  - Final commercial alloy for cladding applications will likely contain Mo for solid solution strengthening, in addition to increased impurities and other additions
- Quantify α′ microstructures in ODS variants and correlate defect structures to mechanical testing results
- Study ODS precipitate stability under continued ion irradiation
  - Increases understanding of dose rate effects and ability to simulate neutron irradiation damage with ion irradiation experiments

Acknowledgements
The author would like to personally thank K.G. Field, P.D. Edmondson, K. Sridharan, K.C. Littrell, R.H. Howard, Y. Yamamoto, S. Dryepondt, and K. Hattar for their contributions to this work. Research was sponsored by the U.S. DOE's Office of Nuclear Energy, Advanced Fuel Campaign of the Fuel Cycle R&D Program and the U.S. DOE's Office of Science, Fusion Energy Sciences. Research on the CG-2 General Purpose SANS at ORNL's HFIR was sponsored by the Scientific User Facilities Division, Office of Basic Energy Sciences, U.S. DOE and research on the Cameca LEAP 4000X HR housed at the Center for Advanced Energy Studies (CAES) and ORNL was sponsored by the National Scientific User Facility (NSUF) and the Center for Nanomaterials Science (CNMS), respectively. This research was performed, in part, using instrumentation (FEI Talos F200X TEM) provided by the Department of Energy, Office of Nuclear Energy, Fuel Cycle R&D Program, and the Nuclear Science User Facilities. Sandia National Laboratories is a multimission laboratory managed and operated by National Technology and Engineering Solutions of Sandia, LLC., a wholly owned subsidiary of Honeywell International, Inc., for the U.S. Department of Energy's National Nuclear Security Administration under contract DE-NA0003525.

References

[1] B.A. Pint, et al., *Journal of Nuclear Materials* **440**, 420 (2013).
[2] G. Bonny, D. Terentyev, & L. Malerba, *Scripta Materialia* **59**, 1193 (2008).
[3] Y. Yamamoto, et al., *Journal of Nuclear Materials* **467**, 703 (2015).
[4] S. Dryepondt, et al., ORNL Technical Report, ORNL/TM-2015/539 (2015).
[5] C.M. Parish, et al., *Journal of Materials Research* **30**, 1275 (2015).
[6] I.M. Lifshitz & V.V. Slyozov, *Journal of Physics and Chemistry of Solids* **19**, 35 (1961).
[7] K.G. Field, et al., *Journal of Nuclear Materials* **465**, 746 (2015).
[8] P.D. Edmondson, et al., *Scripta Materialia* **116**, 112 (2016).
[9] S.A. Briggs, et al., *Acta Materialia* **129**, 217 (2017).